NIMROD CDX-U Update and Other Developments

Carl Sovinec

University of Wisconsin-Madison

and the NIMROD Team

CEMM Collaboration Meeting

Orlando, Florida

November 11, 2007

Topics

- CDX-U Update: nothing to report, but …
- Reconnection computations
  - Tearing mode
  - GEM and driven reconnection
  - Cylindrical benchmark
- Preconditioning
- SuperLU interface

Reconnection Computations: tearing mode

J. King has extended large guide field linear computations for benchmarking with theory by V.V. Mirnov. [GP8.00143]

δ/L	Γ (NIMROD)	Γ (Theory)	Error (%)
0.12	7.48E-004	8.05E-004	7.6
0.09	4.93E-004	5.10E-004	3.44
0.08	3.48E-004	3.61E-004	3.53
0.05	1.61E-004	1.61E-004	0.49

Box Size	1 m
L	0.1667 m
ρ_s	0.1205 m
β	0.1
Δ'	1.66 m^{-1}

Reaching the asymptotic regime with $\rho_s < L$ and $L <<$ box requires greater resolution (packed 120×14, biquartic) than previous cases with $L < \rho_s$. Table shows small delta-prime, large-beta regime results.

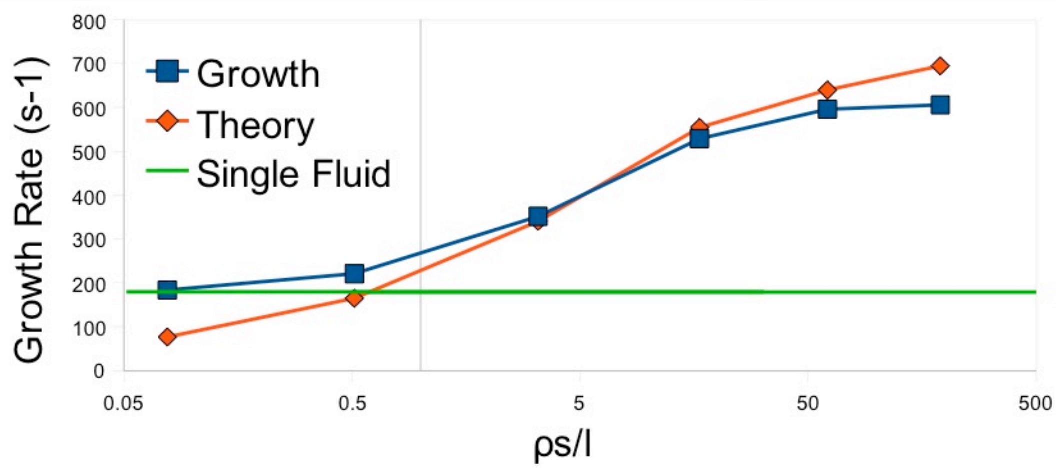

Box Size	1 m
L	0.1667 m
δ	~3 x 10^{-2} m
Δ'	1.66 m^{-1}
S	1.33 x 10^{5}

NIMROD results transition to MHD behavior in the small ρ_s limit. The theory assumes a two-fluid ordering and does not match in this limit.

Tearing mode (continued)

• A scan to large Δ' is inconclusive so far. Simulation results approach the MHD limit, and we have a discrepancy in evaluating the analytical prediction.

• Cylindrical benchmarks are being performed for core and edge tearing modes in RFP equilibria.

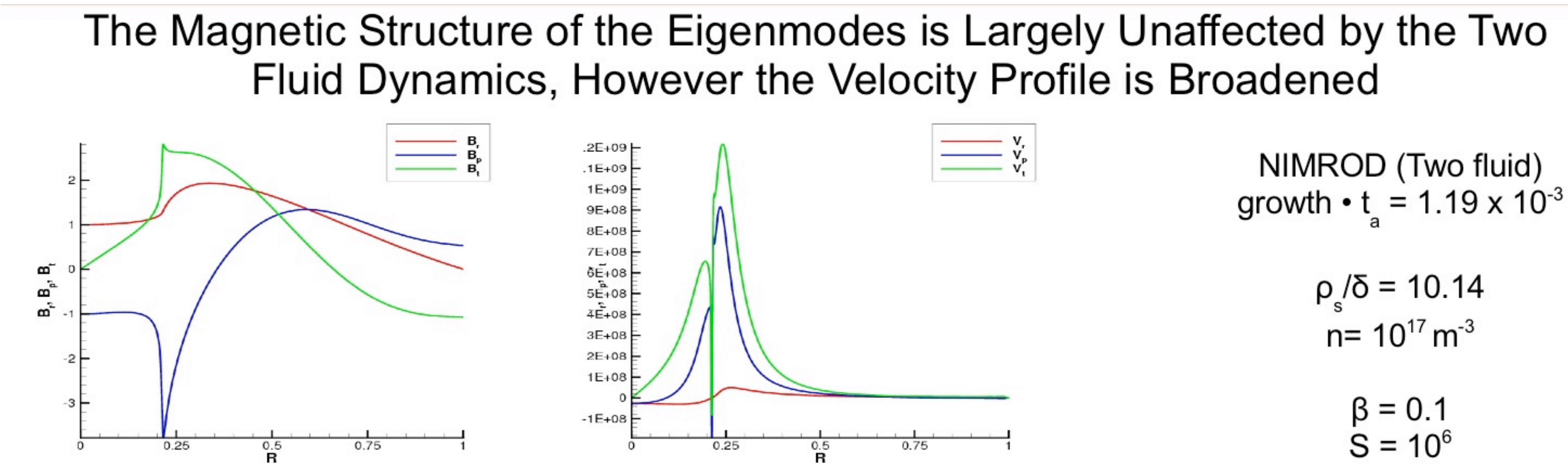

• We are also investigating stabilization from non-equilibrium rotation.

• Nonlinear computations (now also with $\rho_s < L$) will be extended to consider multiple helicities in slab and cylindrical geometry.

GEM Computations

The GEM problem set-up is artificial, but it has become a standard test case.

• The equilibrium has a current sheet and density profile width of order 1 ion skin depth.

• The box size is 12.8×25.6 d_i.

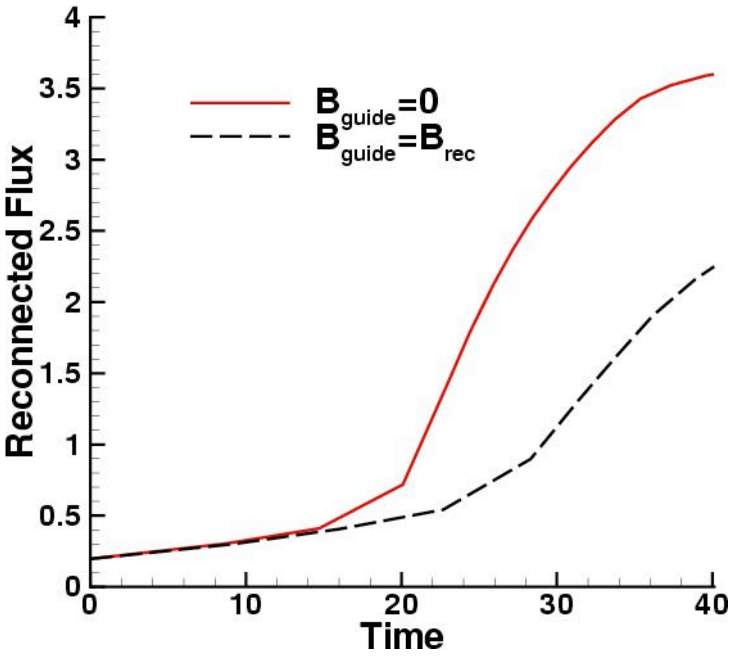

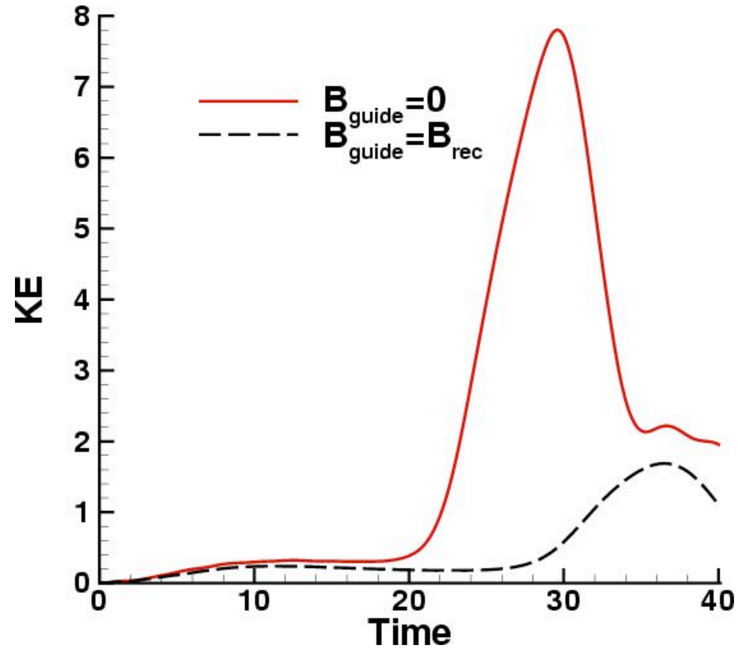

• Adding guide field damps the two-fluid effect, in agreement with M3D-C1.

We have found that electron inertia with m_e=0.01m_i facilitates the magnetic advance, and we are able to reduce artificial particle diffusivity.

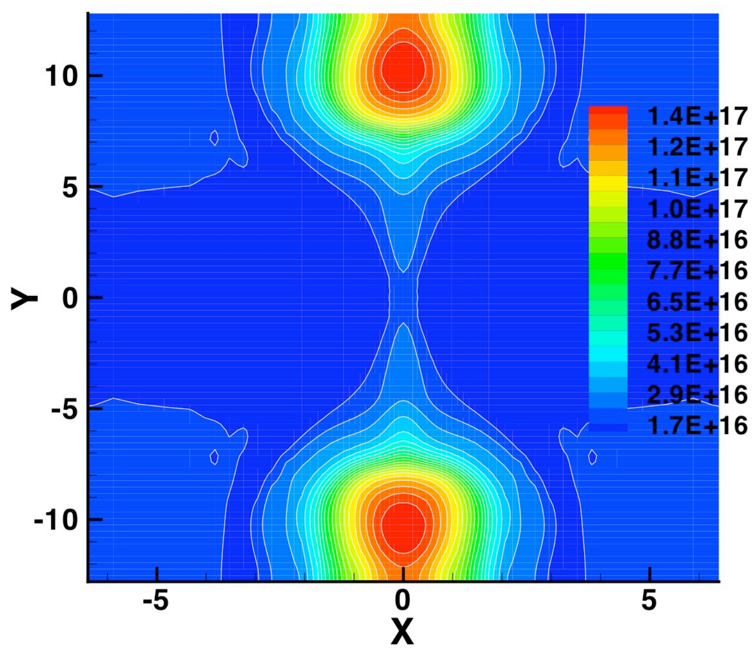

No guide-field case at $\Omega_i t$=28 and D=5×10^{-4}.

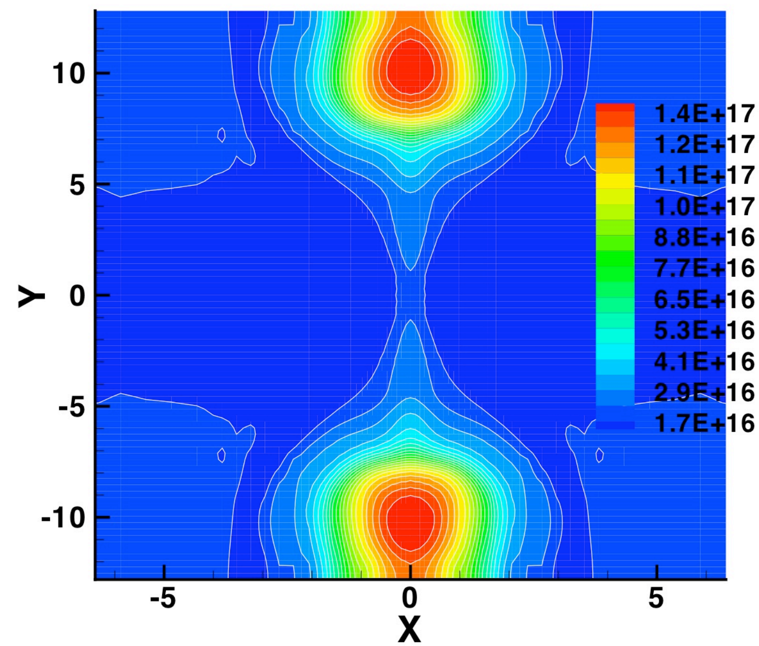

No guide-field case at $\Omega_i t$=28 and D=5×10^{-5}.

Reducing *D* changes the maximum kinetic energy by 1% with or without guide-field. The timing of the peak is a little more sensitive with guide-field than it is without.

MRX Simulation

N. Murphy is investigating the role of geometry in driven reconnection in the MRX experiment using realistic parameters. [TP8.00013]

• With MHD, current sheets are limited by flux-core separation.

• Pressure from outflow tends to build-up in both MHD and two-fluid modeling.

• Toroidal geometry is significant in that the two volumes available for outflow (inflow) differ with push (pull) reconnection.

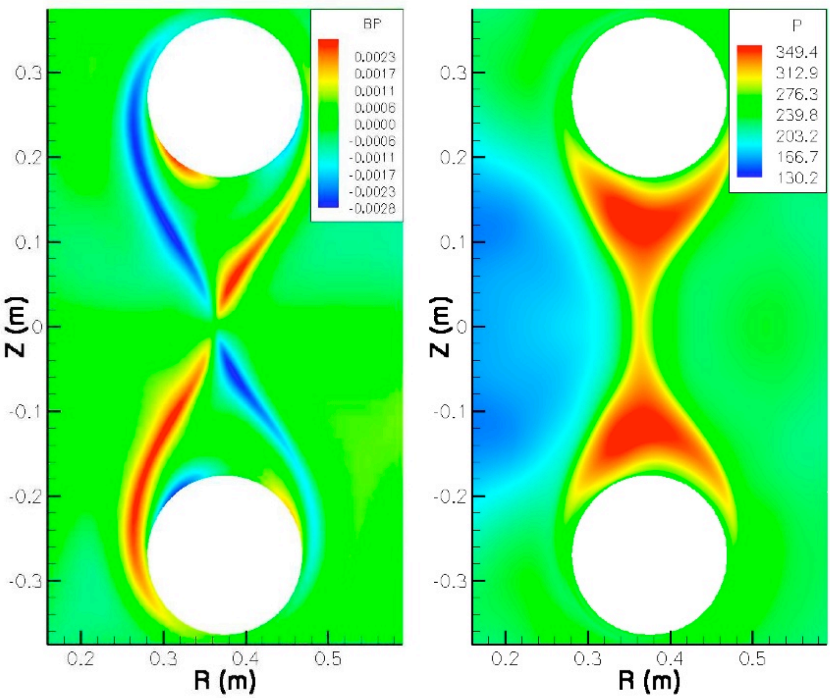

Out-of-plane component of B (left) and pressure (right) from a 2D two-fluid MRX simulation show asymmetry due to geometry.

Cylindrical sawtooth start:

• Using non-reduced modeling, Germaschewski's MRC code has reproduced the Aydemir 4-field result of nonlinear non-exponential growth for the cylindrical 1/1. [Aydemir, PF B 4, 3469 (1992)]

Parameters from the reference:

$$S = \tau_r / \tau_{Hp} = 10^6 \quad \tau_r \equiv \mu_0 a^2 / \eta \quad \tau_{Hp} \equiv a\sqrt{\mu_0 \rho} / B_p$$

$$\beta = 5 \times 10^{-3} \quad \delta = d_i / 2 = 0.11$$

Calculations reported here also use:

$$\mu_0 \nu_{iso} / \eta = \mathrm{Pm} = 0.1 \quad \mu_0 D / \eta = 0.01 \quad T_i \cong 0$$

• Aydemir's resistive MHD case has $\gamma_{MHD}\tau_{Hp}$=0.01.

• With a flat pressure profile and $q(r)=0.98+0.51(r/a)^2$ has the 1/1 resonant surface at r=0.2a.

• NIMROD produces $\gamma_{MHD}\tau_{Hp}$=0.0183 and $\gamma_{2fl}\tau_{Hp}$=0.0207.

• Computations have been performed with r-θ and r-z meshes.

• Spatial resolution for MHD has been varied from 16×18 bicubic, 0≤m≤2 to 48×48 biquartic, 0≤m≤10.

Achieving numerical convergence of the fluctuation energy does not require a lot of resolution for MHD modeling, but ripples in density appear during saturation.

Magnetic fluctuation histories (natural log) for a 32x48 bicubic computation (left) and a 48x48 biquartic computation (right).

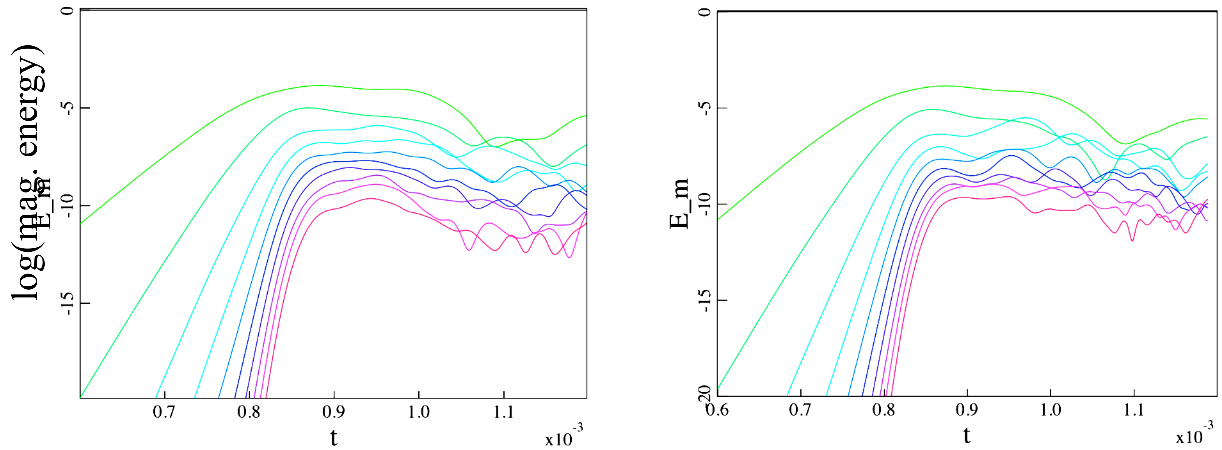

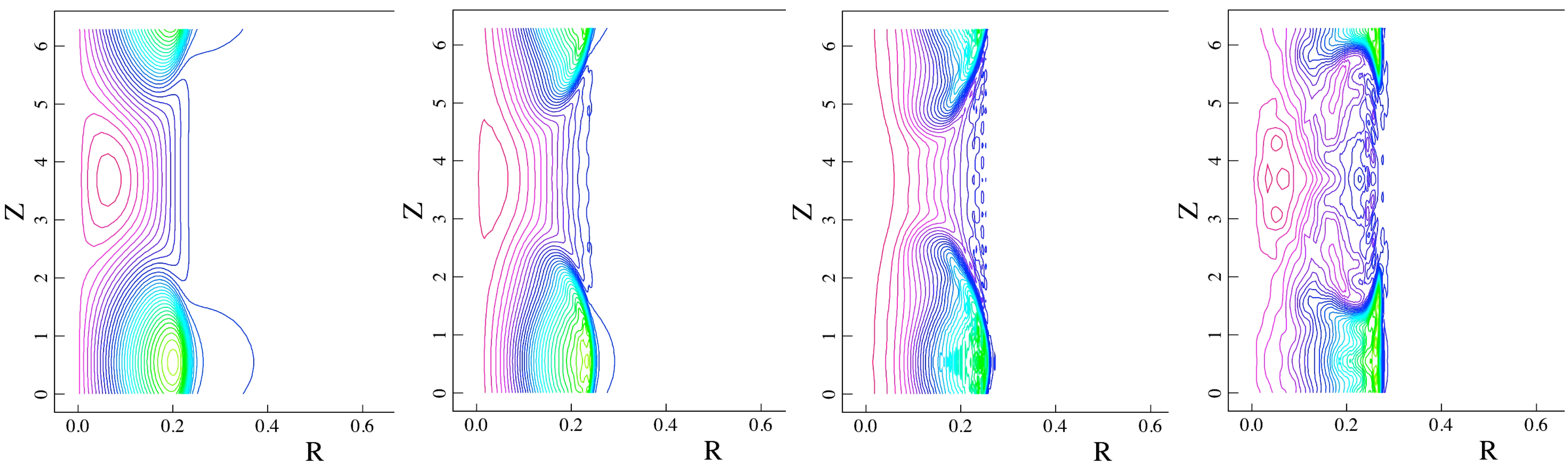

Contours of constant number density for the bicubic computation at 840, 890, 950, and 1200 τ_{Hp}.

Two-fluid computations need improved preconditioning.

- The only two-fluid computation to run through saturation has low resolution (14×12 biquartics, $0 \le n \le 2$).
- At this low resolution, there is no evidence of an increasing 1/1 growth rate at reconnection.

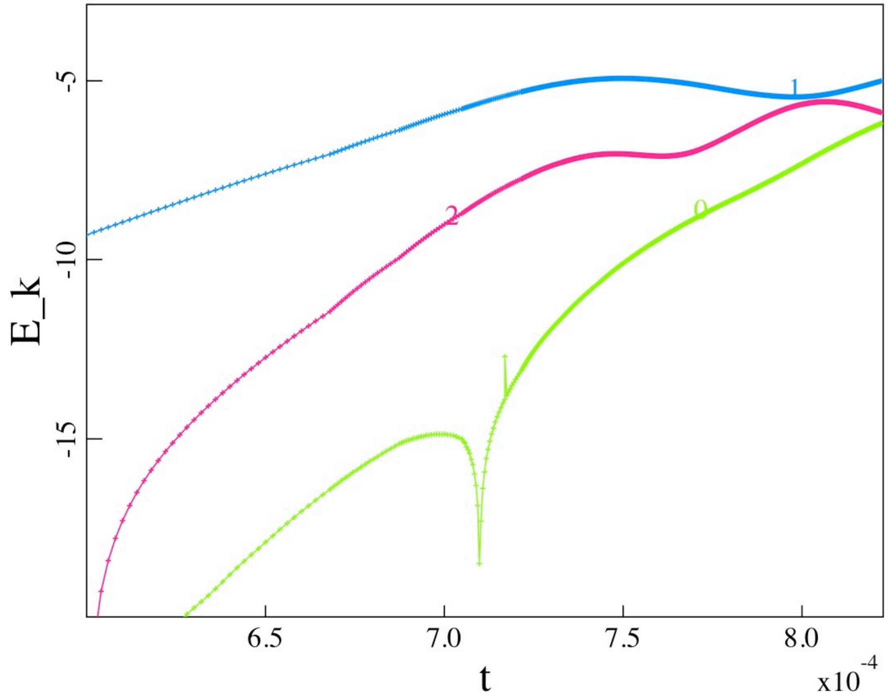

Natural log of kinetic fluctuation energy.

Preconditioning: Even a small nonlinear calculation shows that toroidal relaxation is needed for the two-fluid model.

- A computation with a 14×12 mesh of biquartic elements for the *r*-*z* plane and 3 Fourier components takes 40+ GMRES its with SLU preconditioning.
- Test case: 6×6 bicubic and a large initial perturbation of bamp=0.01.
- GMRES its for the HMHD B-advance on restarts after four steps:
  - With 3D n, $\mathbf{B}^{j+1/2}$, $\mathbf{J}^{j+1/2}$, and $\mathbf{V}^{j+1/2}$ coefficients: 58
  - With $\phi-$ averaged $\mathbf{B}^{j+1/2}$: 30
  - With $\phi-$ averaged $\mathbf{B}^{j+1/2}$ & $\mathbf{J}^{j+1/2}$: 29
  - With $\phi-$ averaged $\mathbf{B}^{j+1/2}$ & $\mathbf{J}^{j+1/2}$; continuity="n=0 only": 7
  - With $\phi-$ averaged $\mathbf{B}^{j+1/2}$, $\mathbf{J}^{j+1/2}$ & $\mathbf{V}^{j+1/2}$; "n=0 only": 5
- GMRES orthogonalization accuracy was checked.

$$\frac{\Delta\mathbf{B}}{\Delta t}-\frac{1}{2}\nabla\times\left(\mathbf{V}^{j+1}\times\Delta\mathbf{B}\right)+\frac{1}{2}\nabla\times\frac{1}{\overline{n}e}\left(\mathbf{J}^{j+1/2}\times\Delta\mathbf{B}+\Delta\mathbf{J}\times\mathbf{B}^{j+1/2}\right)+\frac{1}{2}\nabla\times\eta\Delta\mathbf{J}$$

Left side of B-advance.

Toroidal preconditioning requires another approximate matrix that can be inverted relatively easily.

- Poloidal and toroidal operations can be applied sequentially

  $AM^{-1}v \rightarrow AM_{pol}^{-1}M_{tor}^{-1}v$ or $AM_{tor}^{-1}M_{pol}^{-1}v$ or additively.

- FFTs will at least be used to transform the operand and resultant vectors.

- Finite differences in toroidal angle may provide a useful approximation for the spectral derivatives, leading to tridiagonal or block-tridiagonal matrices over toroidal angle.

- NIMROD's layer parallelism and domain swapping will work.

- A module of utility functions and some simple operations based on 1D-in-ϕ-like equations have been started.

- Limited poloidal coupling may be incorporated if needed.

SuperLU Interface

• To save memory, sets of matrix rows are completed on each processor using point-to-point communication.

• The implementation now allows a choice of either the distributed-memory or the full-storage interface to SLU_DIST.

• Full-storage implementation has also been improved by replacing many large allreduce calls with point-to-point plus allgather operations.

• The changes facilitate intefacing to PETSc--Vadlamani has run both SLU and MUMPS on real systems.

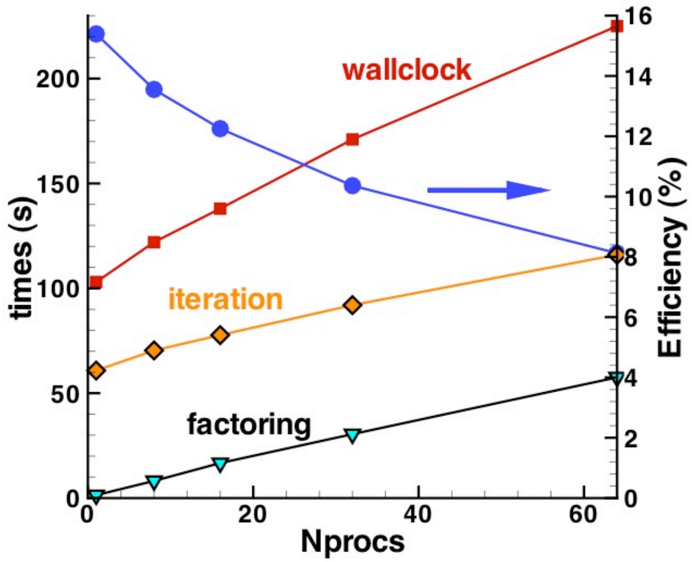

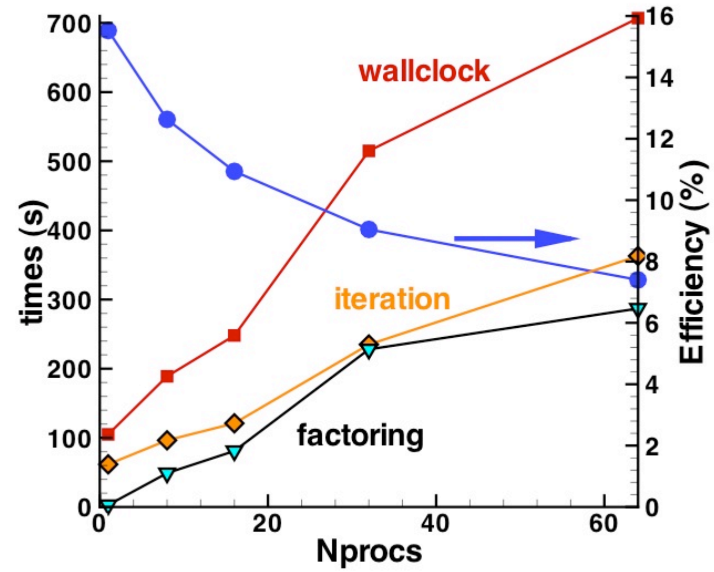

• Timings on the left show weak scaling with the revised full-storage interface.

• Timings with the distributed-memory interface and reordering are essentially identical.

• Timings on the right represent the distributed-memory interface without reordering.

List of NIMROD Presentations at APS '07

Invited:

1. D.C. Barnes Closure of computational fluid models with evolving-background δf kinetics, Session BI2: 9:30 AM-12:30 PM, Monday
2. V.A. Izzo MHD simulations of disruption mitigation on DIII-D and Alcator C-Mod, Session UI1: MHD 2:00-5:0PM, Thursday

Contributed:

3. Christopher Carey BP8.00106 MHD kink instability driven by differential rotation
4. E.B. Hooper CP8.00036 Predictive capability for whole-device spheromak MHD physics
5. R. Jayakumar CP8.00037 Linear MHD Stability Analysis of the SSPX Spheromak
6. Lynda LoDestro CP8.00039 Flux amplification in SSPX
7. Cihan Akcay CP8.00053 Nimrod Simulations of Decaying and Driven HIT-SI Plasmas
8. Scott Parker CP8.00107 A Low Moment Kinetic MHD Simulation Model
9. R. Takahashi GP8.00099 Kinetic Effects of a Non-Maxwellian Distribution of Energetic Particles on 2/1 Stability
10. Thomas G. Jenkins GP8.00122 Progress in theoretical and numerical modeling of RF/MHD coupling using NIMROD
11. B.A. Nelson GP8.00131 Results from the PSI-Center Interfacing Group
11. J.R. King GP8.00143 Numerical Studies of Linear Two Fluid Tearing Modes in Slab and Cylindrical Geometries
12. R.D. Milroy GP8.00133 The Effect of a Weak Toroidal Field on the n=2 Rotational Instability in an FRC
13. R.A. Bayliss GP8.00134 Nonlinear MHD simulation of DC helicity injection in spherical tokamaks
14. Charlson C. Kim GP8.00135 Impact of velocity space distribution on hybrid kinetic MHD simulation of the (1,1) internal kink mode
15. Eric Held GP8.00137 Time-dependent closures for plasma fluid equations
16. J.M. Reynolds JP8.00140 Numerical Simulation of Pulsed Parallel Current Drive in RFPs
17. S. Woodruff PP8.00115 Comparative study of two methods for compressing compact tori: liquid liners and traveling waves
18. A.Y. Pankin TO3.00007 Self-consistent Modeling of the Pedestal in Tokamak H-mode Plasmas
19. Nicholas Murphy TP8.00013 Global Two-Fluid Simulations of Magnetic Reconnection
20. S.E. Kruger UP8.00025 Modeling of the Plasma Response to Resonant Magnetic Perturbations with the NIMROD Code
21. Jeong-Young Ji UP8.00014 Moment approach to the derivation of diffusive and general parallel closures